



POLİTEKNİK DERGİSİ

JOURNAL of POLYTECHNIC

ISSN: 1302-0900 (PRINT), ISSN: 2147-9429 (ONLINE)

URL: <http://dergipark.org.tr/politeknik>



Ecotoxicity study of iron oxide nanoparticles on *Chlorella* sp. and *Daphnia magna*

Chlorella sp. ve *Daphnia magna* üzerinde demir oksit nanopartiküllerinin ekotoksisite çalışması

Yazar(lar) (Author(s)): Burcu ERTİT TAŞTAN¹, İlknur KARS DURUKAN², Mehmet ATEŞ³

ORCID¹: 0000-0003-4644-8305

ORCID²: 0000-0001-5697-0530

ORCID³: 0000-0002-2764-6579

Bu makaleye şu şekilde atıfta bulunabilirsiniz (To cite to this article): Ertit Taştan B., Kars Durukan İ. ve Ateş M., “Ecotoxicity study of iron oxide nanoparticles on *Chlorella* sp. and *Daphnia magna*”, *Politeknik Dergisi*, 23(4): 1073-1079, (2020).

Erişim linki (To link to this article): <http://dergipark.org.tr/politeknik/archive>

DOI: 10.2339/politeknik.581107

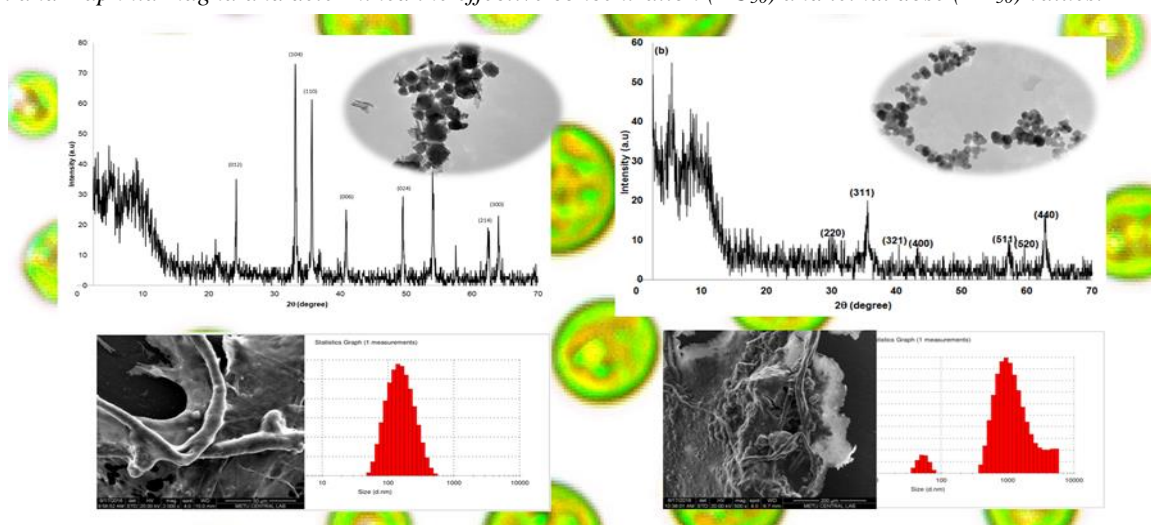
Ecotoxicity Study of Iron Oxide Nanoparticles on *Chlorella* sp. and *Daphnia magna*

Highlights

- ❖ Acute toxicity of α -Fe₂O₃ and γ -Fe₂O₃ nanoparticles on two aquatic species were tested.
- ❖ The EC₅₀ concentration was 500 mg/L for α -Fe₂O₃ treated *Daphnia magna*
- ❖ The LD₅₀ concentration was 1000 mg/L for α -Fe₂O₃ treated *Daphnia magna*
- ❖ Increasing NPs concentrations caused to decrease of *Chlorella* sp. growth
- ❖ Increasing NPs concentrations did not show completely toxic effect of *Chlorella* sp.

Graphical Abstract

The study investigated the impacts of α -Fe₂O₃ and γ -Fe₂O₃ NPs on behavioral change and ecotoxicity of *Chlorella* sp. and *Daphnia magna* and determined the effective concentration (EC₅₀) and lethal dose (LD₅₀) values.



Aim

The aim of the current study was to investigate the effects of α -Fe₂O₃ and γ -Fe₂O₃ NPs on aquatic organisms; *Chlorella* sp. and *D. magna*.

Design & Methodology

α -Fe₂O₃ and γ -Fe₂O₃ NPs were analyzed by XRD, TEM, DLTS and Zeta potential

Originality

The effects of particle size and solubility were comparatively examined on the toxicity of α -Fe₂O₃ and γ -Fe₂O₃ NPs to *Chlorella* sp. and *D. magna*. in aquaculture.

Findings

Increasing α -Fe₂O₃ and γ -Fe₂O₃ NPs concentrations caused to decrease of microalgal growth but did not show completely toxic effect. The EC₅₀ concentration value was 500 mg/L and LD₅₀ concentration value was 1000 mg/L for α -Fe₂O₃ treated daphnids in 72 h, respectively.

Conclusion

The paper demonstrates the significant evidence in understanding acute toxicity of iron oxide nanoparticles for environmental protection as part of risk assessment strategies.

Declaration of Ethical Standards

The authors of this article declare that the materials and methods used in this study do not require ethical committee permission and/or legal-special permission.

Chlorella Sp. ve Daphnia Magna Üzerinde Demir Oksit Nanopartiküllerinin Ekotoksosite Çalışması

Araştırma Makalesi / Research Article

Burcu ERTİT TAŞTAN¹, İlknur KARS DURUKAN^{2*}, Mehmet ATEŞ³

¹Sağlık Hizmetleri Meslek Yüksek Okulu, Dişçilik Hizmetleri Bölümü, Gazi Üniversitesi, Türkiye

²Fen Fakültesi, Fizik Bölümü, Gazi Üniversitesi, Türkiye

³Mühendislik Fakültesi, Biyomühendislik Bölümü, Munzur Üniversitesi, Türkiye

(Geliş/Received : 21.06.2019 ; Kabul/Accepted : 16.10.2019)

ÖZ

Nanopartiküller, bir çok endüstriyel alanda kullanımları nedeniyle büyük öneme sahiptirler. Ancak, büyük çapta kullanımları neticesinde sucul ortamlar üzerinde toksisiteye neden olmaktadır ve bu etkileri detaylı analizlerle henüz açıkça anlayamamaktadır. Demir oksit nanoparçacıkları (Fe_2O_3 NP'ler) birçok endüstride yaygın olarak kullanılmaktadır ve sularda yaşayan türler için oldukça toksik olarak kabul edilmektedirler. Bu makale iki sucul tür üzerindeki $\alpha-Fe_2O_3$ ve $\gamma-Fe_2O_3$ NP'lerinin akut toksisitesini göstermektedir. $\alpha-Fe_2O_3$ ve $\gamma-Fe_2O_3$ 'ün çeşitli konsantrasyonlarının (0, 50, 100, 250, 500 ve 1000 mg / L) *Chlorella* sp. ve *D. magna* üzerindeki etkileri araştırılmıştır. Çalışmada mikroalgal gelişimin, $\alpha-Fe_2O_3$ ve $\gamma-Fe_2O_3$ NP konsantrasyonlarının artmasıyla azaldığı, ancak önemli bir toksik etki göstermediği belirlenmiştir. Ayrıca 72 saat $\alpha-Fe_2O_3$ ile muamele edilmiş daphidler için EC50 değeri 500 mg / L ve LD₅₀ değeri 1000 mg /L olarak tespit edilmiştir. Çalışma sonucunda, Fe_2O_3 NP'lerin akut toksisitesinin risk değerlendirmesi çevre korumaya yönelik olarak tüm detaylarıyla belirlenmiştir.

Anahtar Kelimeler: $\alpha-Fe_2O_3, \gamma-Fe_2O_3$, nanoparçacıklar, nanotoksosite, *Chlorella* sp., *Daphnia magna*.

Ecotoxicity Study of Iron Oxide Nanoparticles on *Chlorella* Sp. and *Daphnia Magna*

ABSTRACT

Nanoparticles have great impact due to their tremendous industrial applications. However, their applications have produced toxicity effects on the aquatic environments and their detailed analyses are not clearly understood. Iron oxide nanoparticles (Fe_2O_3 NPs) are being used extensively in many industries but are considered highly toxic to aquatic species residing in surface waters. This paper demonstrates the acute toxicity of $\alpha-Fe_2O_3$ and $\gamma-Fe_2O_3$ NPs in two aquatic species. The effects of various concentration (0, 50, 100, 250, 500 and 1000 mg/L) of $\alpha-Fe_2O_3$ and $\gamma-Fe_2O_3$ on the sensitivity response of the *Chlorella* sp. and *D. magna* were investigated. The growth of microalgal decreased with increased concentration of the $\alpha-Fe_2O_3$ and $\gamma-Fe_2O_3$ NPs concentrations but did not show a significant toxic effect. The EC₅₀ concentration value was 500 mg/L and LD₅₀ concentration value was 1000 mg/L for $\alpha-Fe_2O_3$ treated daphnids in 72 h, respectively. The findings demonstrate the significant evidence in understanding acute toxicity of Fe_2O_3 NPs for environmental protection as part of risk assessment strategies.

Keywords: $\alpha-Fe_2O_3, \gamma-Fe_2O_3$, nanoparticles, nanotoxicity, *Chlorella* sp., *Daphnia magna*.

1. INTRODUCTION

Metal oxide nanoparticles are attracting great interest due to their tremendous applications in engineering, water treatment, medicine and cosmetics (1). Among these oxides, iron oxides are very important materials, composed of three different forms: hematite ($\alpha-Fe_2O_3$), maghemite ($\gamma-Fe_2O_3$), and magnetite (Fe_3O_4) (2). $\alpha-Fe_2O_3$ is a thermo dynamically stable structure at ambient conditions. It has more rigid structure than diamond and offers high resistance to corrosion. Additionally, it is low cost (3, 4). $\gamma-Fe_2O_3$ is magnetic, which has an isometric crystalline structure. At room temperature, $\gamma-Fe_2O_3$ is ferromagnetic, but if smaller than 10 nm, they are considered as super paramagnetic. At high temperature,

$\gamma-Fe_2O_3$ is unstable and loses its sensitivity over time. Iron oxide nanomaterials are widely used in drug delivery (5), biosensing (6), cell labeling (7), magnetic trapping (8), and magnetic resonance imaging (9), biomolecular-magnetic hyperthermia (10). Iron oxide nanomaterials are generally regarded as non- or low-toxic (11-13). However, recent studies have revealed that iron oxide nanomaterials have potential adverse effects due to their potential escape into the environment (14). Super paramagnetic iron oxide nanoparticles show less cytotoxicity (15-17) also found that ferric oxide nanoparticles have produced potential lung and systemic cumulative toxicity in rats, and intravascular iron oxide nanoparticles that may induce human endothelial inflammation and dysfunction. Moreover, iron oxide nanomaterials could serve as significant carriers of toxic chemicals (18; 19) and increase exposures to adsorbed

*Sorumlu Yazar (Corresponding Author)
e-posta : ilknurdurukan@gazi.edu.tr

pollutants. An acute toxicity of citrate coated Fe₃O₄ NP was reported as 57.1 mg/L (48-EC₅₀) and 31.7 mg/L (96-EC₅₀) for *Daphnia magna* (*D. magna*), which were partially ascribed to dissolved iron ions and their ability to form reactive oxygen species (ROS) (20). The fate, transport and exposure pathways of manufactured Fe₃O₄NP were also investigated using pumpkin plants (*Cucurbita maxima*) (21). Additionally, a previous study was reported on the effects on the Fe₂O₃(≥10 mg/L) NP on the development of mental toxicity of zebrafish (*Danio rerio*) embryos was studied on mortality, hatchingdelay, and malformation (22). Apart from that, another study was reported the toxic effects of Fe₃O₄ nanoparticles (35 nm) on the green alga *Chlorella vulgaris* treated 72 h to a nominal concentration range from 200 to 1600 µg/mL. In a previous paper, the authors showed an induction of oxidative stress and an alteration of photosynthetic activity based on absorbed CO₂ fixation (22). Similarly, the toxicity of super paramagnetic iron oxide nanoparticles was investigated on *Chlorella vulgaris* cells exposed during 72 hours to Fe₃O₄ to a range of concentrations from 12.5 to 400 µg/mL. Under these treatments, toxicity impact was indicated by the deterioration of photochemical activities of photosynthesis, the induction of oxidative stress, and the inhibition of cell division rate.

The aim of the current study was to investigate the effects of α-Fe₂O₃ and γ-Fe₂O₃ NPs on aquatic organisms; *Chlorella sp.* and *D. magna*. These species are chosen since they are widely used as food in aquaculture and they are two of the most frequently used species in aquaculture (23). We investigated the impacts of α-Fe₂O₃ and γ-Fe₂O₃ NPs on behavioral change and ecotoxicity, and determined the effective concentration (EC₅₀) and lethal dose (LD₅₀) values. The attachment and accumulation of α-Fe₂O₃ and γ-Fe₂O₃ NPs in aquatic organisms were investigated using scanning electron microscopy (SEM). Also the effects of particle size and solubility were comparatively examined on the toxicity of α-Fe₂O₃ and γ-Fe₂O₃ NPs to these commonly used phytoplankton and zooplankton species in aquaculture.

2. MATERIAL VE METHOD

2.1 Nanoparticle Characterization

The characteristic feature of nanomaterials, such as size, shape, size distribution, surface area, solubility, aggregation, etc. need to be evaluated before assessing toxicity or biocompatibility (24). Morphologies of the α-Fe₂O₃ and γ-Fe₂O₃ NPs were examined using transmission electron microscopy (TEM), Powered X-ray diffraction analysis (XRD) was carried out to characterize the crystal structure of the NPs. Hydrodynamic diameters and zeta potentials of the NPs were measured with a Zetasizer (25, 26).

2.2 Microalgae culture conditions

The microalgae *Chlorella sp.* was isolated from the water supply in Sorgun, Yozgat, Turkey (27). The medium BG 11 (28) was used to conduct algal growth inhibition assay

based on the OECD 201 (29). The starting OD value of microalgal cultures in the beginning of the experiments was about 0.2 in 100 mL BG11 media in 250 mL Erlenmayer flasks at 25 ± 2 °C under continuous illumination at 25 µmol/m²s (1750 lx) at 100 rpm stirring rate.

D. magna, a planktonic crustacean was used as test species (30). The daphnids were maintained at a constant temperature of 20 ± 1 °C at 16:8 h light:dark cycle. The acute immobilization test was based on the OECD 202 (31).

2.3 Microalgal Growth Inhibition

Exponentially growing algal cells were propagated in Erlenmayer flasks containing α-Fe₂O₃ and γ-Fe₂O₃ at 50, 100, 250, 500 and 1000 mg/L of the BG11 medium separately. In addition, the control medium consisted of flasks without α-Fe₂O₃ or γ-Fe₂O₃ NPs. All experiments were carried out twice in triplicate.

2.4 Acute Immobilization

D. magna, a planktonic crustacean was used as test species [30]. The daphnids were maintained at a constant temperature of 20 ± 1 °C at 16:8 h light:dark cycle. The acute immobilization test was based on the OECD 202 (31). Increasing concentrations of α-Fe₂O₃ or γ-Fe₂O₃ NPs at 0, 50, 100, 250, 500 and 1000 mg/L were prepared in the ISO test medium to determine the sensitivity response of *D. magna*. A total of 5 daphnids were put in 3 replicates for each concentration tested. Following the 24, 48 and 72 h exposures, daphnids were studied for immobilization effects, with simultaneous comparison with controls.

2.5 Analytical Methods

Cell growth of *Chlorella sp.* was determined by measuring optic density, dried cell mass and specific growth rate parameters for any set of growth conditions. Optic density was measured at 600 nm with Shimadzu UV 1800 model spectrophotometer. The dried cell mass was calculated by the measurement of pellets, which were dried at 80 °C for overnight (Nüve FN 400 model sterilizator) after centrifugation step (3421x g = 5000 rpm for 10', Hettich Universal 320R model centrifuge). The chlorophyll concentrations were determined according the method developed by (32) at 646.6 nm for chlorophyll *a* and at 663.6 nm chlorophyll *b*. The chlorophyll concentrations were expressed in µg of chlorophyll per milliliter.

Specific growth rate (µ) was calculated according to the equation (1) (33);

$$\mu = (\ln X_2 - \ln X_1) \div (t_2 - t_1) \quad (1)$$

where X₂ and X₁: dry cell weight concentrations (g/L) at time t₂ and t₁, respectively. Maximum biomass productivity was calculated according to the equation (2);

$$P_{max} = (X - X_0) \div (t - t_0) \quad (2)$$

where X: final and X₀: initial biomass concentrations (g/L), t: final and t₀: initial time of the culture.

Scanning electron microscopy was used to observe the morphology of *Chlorella* sp. as described previously (30).

All of the experiments were performed in triplicate. The standard error of data was calculated according to the equation (3) formulated by (34) where σ represents the square root of the estimated error variance of the quantity.

$$SE = \sqrt{\sigma^2} \quad (3)$$

3. RESULTS AND DISCUSSIONS

3.1 Nanoparticle Characterization

Figure 1 A shows the 2θ -intensity profiles of α -Fe₂O₃ NPs. The data obtained were matched with leptos program, which confirmed the crystalline structure of Fe₂O₃. The XRD diffractograms for α -Fe₂O₃ (hematite) NPs showed 8 peaks within 20-80° range with the

given in JCPDS (24-81) data. This confirms the formation of cubic phase and lattice constant a : 8.35 Å.

The average length and length distribution of the nanoparticles used in our study was determined by transmission electron microscopy. The results of the evaluation of the photographs were calculated as follows: number average diameter (D_p , nm equation (4)) and coefficient of variation for length distributions (CV, % equation (5)). Where N_i determine the number of particles with D_i diameter and SD (equation (6)) determines the standard deviation according to the number average diameter value.

$$D_p = \frac{\sum N_i D_i}{\sum N_i} \quad (4)$$

$$CV = \frac{SD}{D_p} * 100 \quad (5)$$

$$SD = \sqrt{\frac{\sum N_i (D_i - D_p)^2}{(N-1)}} \quad (6)$$

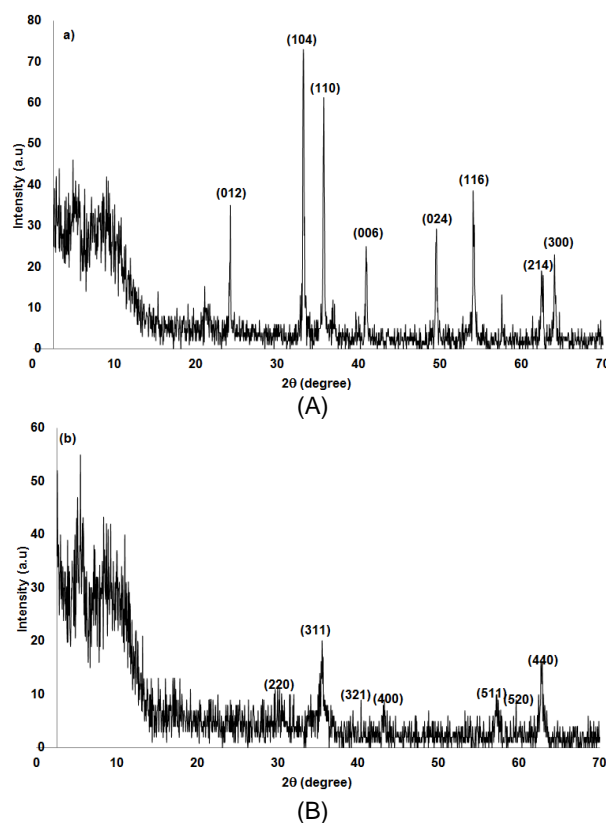


Figure 1. XRD spectrum of α -Fe₂O₃ (A) and γ -Fe₂O₃ (B) NPs.

following hkl values: (012), (104), (110), (113), (024), (116), (214) and (300) and with those given in JCPDS (24-72) data. This confirms the formation of rhombohedral phase and lattice constant a : 5.038 Å and c :13.772 Å. The existence of sharp peaks confirmed that α -Fe₂O₃ NPs were highly crystalline and monodisperse (35)

Figure 1 B shows the 2θ -intensity profiles of γ -Fe₂O₃ NPs. The XRD diffractogram for γ -Fe₂O₃ (maghemite) NPs showed 7 sharp peaks at hkl: (220), (311), (321), (400), (511), (520) and (440). That was consistent with previously published values (36) and also with those

A typical TEM image of α -Fe₂O₃ nanoparticle is given in Figure 2 A. The dispersion of α -Fe₂O₃ nanoparticles have a spherical shape, but also contain structures in the form of nanorods, with a lower concentration. Through the TEM photograph, the average diameter of α -Fe₂O₃ nanoparticles was determined as 57.95 nm, the standard deviation value of length distribution was 23.27 nm, and the coefficient of variation for length distribution was 40 %. However, it should be noted that these values are obtained without taking into account the nanorod form. The γ -Fe₂O₃ NPs TEM image is given in Figure 2 B. As shown in the figure, the average diameter of the γ -Fe₂O₃

nanoparticles was 33.91 nm, the standard deviation value of the length distribution was 8.20 nm, and the coefficient of variation for the length distribution was 24 %. The γ -Fe₂O₃ nanoparticles appear to have spherical morphology, generally spherical morphology, compared to α -Fe₂O₃ nanoparticles.

The TEM, DSL and Zeta Potential (positive / negative charge) analysis values of α -Fe₂O₃ and γ -Fe₂O₃ NPs in the aquatic environment are shown in Table 1. Immediately after ultrasonication the initial sizes of both α -Fe₂O₃ and γ -Fe₂O₃ NPs were found to be 235 nm and 636 nm, respectively. These determined dimensional differences are consistent with zeta potential measurements. In the aquatic environment, an increase in size over time was observed for both NPs. As shown in Table 1, α -Fe₂O₃ and γ -Fe₂O₃ NPs have negatively charged surfaces. Surface loads of suspensions of NPs play an important role in particle stability versus agglomeration in a solvent and in determining interaction with biological systems (37).

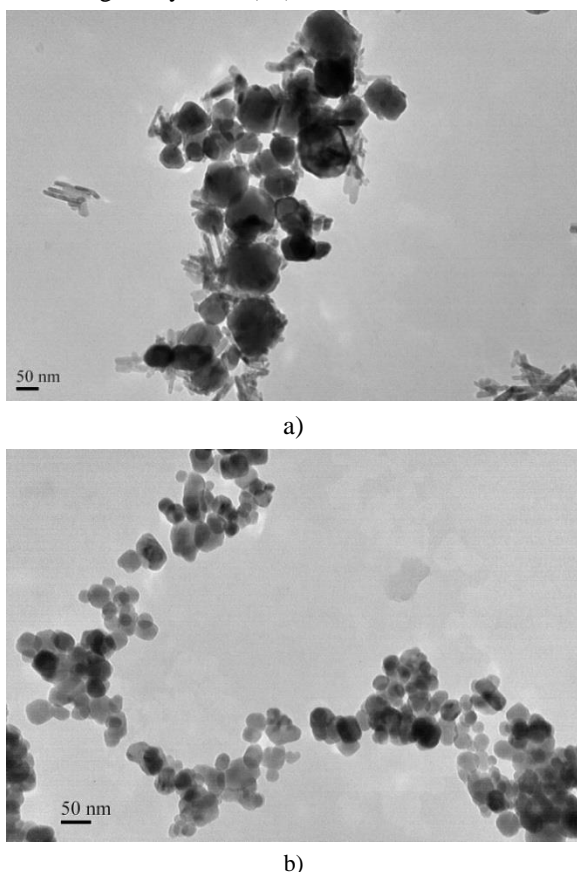


Figure 2. TEM images of α -Fe₂O₃ (a) and γ -Fe₂O₃ (b) NPs.

The Zeta potential value is also used not only as a positive (+) or negative (-) load change on the surface, but also as an indicator of attractive and repulsive forces on the surface. In a recently published study, it is shown that the surface charge of particles in agglutination in water is not sufficient to prevent aggregation of NPs in water even without counter ions, but aggregates were found to be

smaller than other NP studies that were compatible with measured surface loads (38).

Table 1. Size distribution and surface load of α -Fe₂O₃ and γ -Fe₂O₃ NPs in aqueous media

NPs	TEM* (nm)	DLS* (nm)	Zeta*Potential (mV)	Appearance (Color)
α -Fe ₂ O ₃	57.95	235	-2,15	Blurred-yellow
γ -Fe ₂ O ₃	33.91	636	-3.78	Orange

*: Experimental values measured in this study from 10 μ g mL⁻¹ suspensions

The statistical distribution of DLS values in the aquatic environment of NPs is given in Figure 3 A and B. When these graphs are examined, it is seen that α -Fe₂O₃ NPs exhibit fairly steady and stable distribution and γ -Fe₂O₃ NPs exhibit more unstable distribution. All of the metal-based NPs are very unstable in the aquatic environment except for the general situation for NPs, the effects of water on physical and chemical properties in the aquatic environment and tend to aggregate together for various reasons. As a direct consequence of this, they lose their nano properties. Although the size of the aggregate particles is only several times larger than the original particle, the properties exhibited by the material differ. Metal or metal oxide NPs exhibited a similar pattern in our previous studies by our research group (38). In this study, it is seen that γ -Fe₂O₃ NPs in aggregate form more aggregates than α -Fe₂O₃ NPs in freshwater environment.

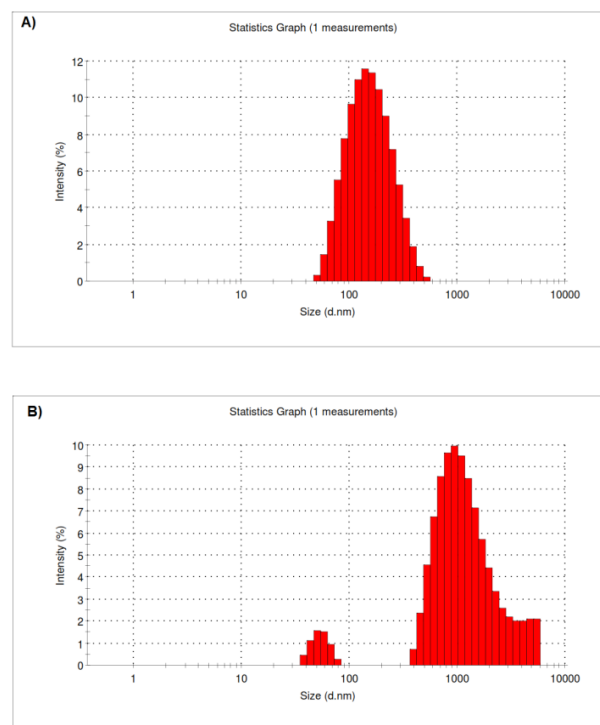


Figure 3. Statistical distribution of DLS values of α -Fe₂O₃ (A) and γ -Fe₂O₃ (B) NPs.

3.2 Toxicity Assessment

3.2.1 Microalgal Growth Inhibition

It was found that the growth inhibition of *Chlorella* sp. is concentration dependent following 72 h of exposure to α -Fe₂O₃ and γ -Fe₂O₃. Initially, during the 72 h observation, it was found that microalgal growth decreased with increasing NPs concentrations (Figure 4). The highest growth was obtained at 50 mg/L α -Fe₂O₃ NP concentration as 0.141 g/L. Dry weight of *Chlorella* sp. decreased from 0.094 g/L to 0.065 g/L when γ -Fe₂O₃ NP concentration increased from 100 mg/L to 1000 mg/L. The α -Fe₂O₃ and γ -Fe₂O₃ concentration at 1000 mg/L showed highly toxic effect on *Chlorella* sp. Thus, it was apparent that increasing α -Fe₂O₃ and γ -Fe₂O₃ NPs concentrations caused to decrease of microalgal growth but did not show completely toxic effect (Table 2).

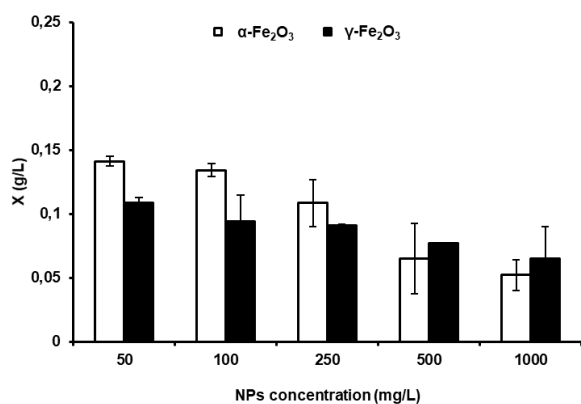


Figure 4. The effect on dry weight (X) of *Chlorella* sp. with α -Fe₂O₃ and γ -Fe₂O₃ NPs during the incubation period.

Chlorophyll (a+b) concentrations of *Chlorella* sp. were also evaluated (Table 2). Following the 72 h exposure, chlorophyll (a+b) concentrations decreased with increasing α -Fe₂O₃ and γ -Fe₂O₃ NPs concentrations.

Calculated P_{max} values are presented in Table 2. As anticipated, 48 h values of productivity at the highest α -Fe₂O₃ and γ -Fe₂O₃ NPs concentrations were lower than the lowest concentrations.

Table 2. α -Fe₂O₃ and γ -Fe₂O₃ NP effect on *Chlorella* sp. Growth parameters during 48 h and 72 h exposures

	50 mg/L	100 mg/L	250 mg/L	500 mg/L	1000 mg/L
α-Fe₂O₃					
X (g/L)	0.141±0.004	0.134±0.005	0.108±0.018	0.065±0.028	0.052±0.012
Pmax ^{48h}	0.0022±0.0001	0.0020±0.0001	0.0018±0.0001	0.0007±0.0001	0.0004±0.0001
μ max ^{48h}	0.028±0.0006	0.027±0.0021	0.030±0.0015	0.0151±0.0008	0.010±0.0002
Chl (a+b)	0.076±0.002	0.072±0.002	0.058±0.0001	0.035±0.0031	0.028±0.006
γ-Fe₂O₃					
X (g/L)	0.109±0.004	0.094±0.021	0.091±0.001	0.077±0.001	0.065±0.025
Pmax ^{48h}	0.0014±0.0001	0.0009±0.0001	0.0008±0.0001	0.0008±0.0001	0.0002±0.0001
μ max ^{48h}	0.020±0.0032	0.014±0.0005	0.011±0.0017	0.010±0.007	0.003±0.001
Chl (a+b)	0.059±0.007	0.050±0.002	0.049±0.0003	0.041±0.0003	0.035±0.003

In a previous paper, results showed the toxicities of 4 zero-valent iron NPs with different sizes to a green alga *Chlorella pyrenoidosa*. The effects of particle size of iron NPs showed that the algal growth inhibition of increased significantly with decreasing particle size (39). These results are similar in ours with the effect of higher toxicity of smaller particle sizes. In our results the size distribution of α -Fe₂O₃ NPs was detected as 57.95 nm in TEM and size distribution of γ -Fe₂O₃ NPs was detected as 33.91 nm. As shown in Table 2 dry weight, P_{max}, μ max and chlorophyll concentrations were lower in the γ -Fe₂O₃ NPs exposed cultures.

Chlorella sp. could be demonstrated as a successful bio indicator in this study and also in many other toxicity studies (39, 40). On the other hand other microalgae species have also been tested in toxicity studies such as *Nannochloropsis* sp. and *Isochrysis* sp. (41).

3.2.2 Acute Immobilization Test

The effects of increasing α -Fe₂O₃ and γ -Fe₂O₃ NPs concentrations on *D. magna* were analyzed during 72 h of exposure. The EC₅₀ concentration value was 500 mg/L and LD₅₀ concentration value was 1000 mg/L for α -Fe₂O₃ treated daphnids in 72 h, respectively (Figure 5 A).

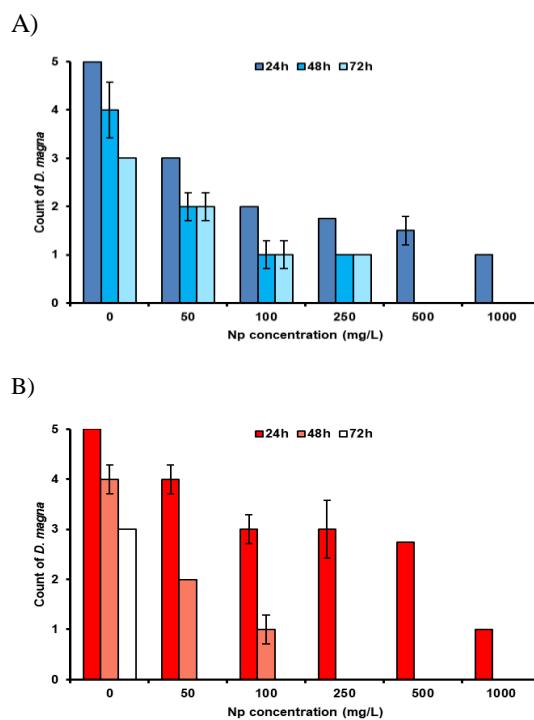
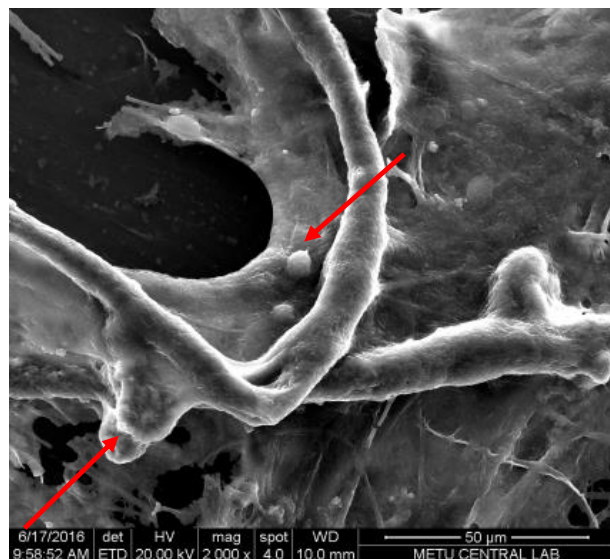


Figure 5. The effect of α -Fe₂O₃ (A) and γ -Fe₂O₃ (B) NP concentrations on *D. magna*.

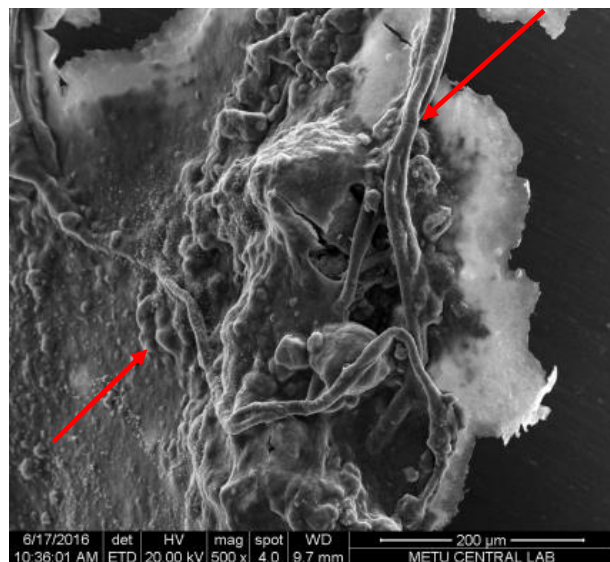
The no observed effect level (NOEL) and low observed effect level (LOEL) were calculated at 0 mg/L and 50 mg/L for γ -Fe₂O₃ at 24 h, respectively. The LD₅₀ concentration value was 50 mg/L γ -Fe₂O₃ NP treated daphnids in 48 h (Figure 5 B).

Further, the SEM images also confirmed to change in morphology (Figure 6). Interestingly, the images indicate

the attachment of α -Fe₂O₃ and γ -Fe₂O₃ NPs on the *Chlorella* sp. caused to aggregation of microalgal cells.



A)



B)

Figure 6. SEM image of *Chlorella* sp. following exposure to α -Fe₂O₃ (A) and γ -Fe₂O₃ (B) NPs (72 h).

4. CONCLUSIONS

In this study, α -Fe₂O₃ and γ -Fe₂O₃ nanoparticles were analyzed by XRD, TEM, DLTS and Zeta potential before toxicity study. The formation of the particles and crystal structure were determined by XRD. The shape, size, length distribution and standard deviation values of the particles with TEM were determined. With DLTS and Zeta potential measurements, particle size distribution, solubility, aggregations were determined. The paper highlighted the acute toxicity of α -Fe₂O₃ and γ -Fe₂O₃ nanoparticles on *Chlorella* sp. and *Daphnia magna*. Increasing α -Fe₂O₃ and γ -Fe₂O₃ NPs concentrations caused to decrease of microalgal growth but did not show completely toxic effect. The EC₅₀ concentration value was 500 mg/L and LD₅₀ concentration value was 1000

mg/L for α -Fe₂O₃ treated daphnids in 72 h, respectively. The paper demonstrates the significant evidence in understanding acute toxicity of iron oxide nanoparticles for environmental protection as part of risk assessment strategies.

ACKNOWLEDGEMENTS

This research is supported by a grant from The Scientific and Technological Research Council of Turkey (TÜBİTAK, Grant No: 114Y087) through TÜBİTAK Center for Department of Bioengineering at Munzur University.

DECLARATION OF ETHICAL STANDARDS

The author(s) of this article declare that the materials and methods used in this study do not require ethical committee permission and/or legal-special permission..

REFERENCES

- [1] Sadiq, I.M., Pakrashi, S., Chandrasekaran, N., Mukherjee, A., "Studies on toxicity of aluminum oxide (Al₂O₃) nanoparticles to microalgae species: *Scenedesmus* sp. and *Chlorella* sp", *J. Nanopart. Res.*, 13: 3287–3299, (2011).
- [2] Fan, H.M., You, G.J., Li, Y., Zheng, Z. Tan, H.R., Shen, Z.X., Tang, S.H., Feng, Y.P., "Shape-controlled synthesis of single-crystalline Fe₂O₃ hollow nanocrystals and their tunable optical properties", *J. Phys. Chem. C*, 113: 9928–9935, (2009).
- [3] Hua, J., Gengsheng, J., "Hydrothermal synthesis and characterization of monodisperse α -Fe₂O₃ nanoparticles", *Mater. Lett.*, 63: 2725–2727, (2009).
- [4] Hsu, L.C., Li, Y.Y., Hsiao, C.Y., "Synthesis, electrical measurement, and field emission properties of α -Fe₂O₃ nanowires", *Nanoscale Res. Lett.* 3: 330–337, (2008).
- [5] Seth, A., Lafargue, D., Poirier, C., Péan, J.M., Ménager, C., "Performance of magnetic chitosan–alginate core–shell beads for increasing the bioavailability of a low permeable drug", *Eur. J. Pharm. Biopharm.*, 8: 374–81, (2014).
- [6] Haun, J.B., Yoon, T.J., Lee, H., Weissleder, R., "Magnetic nanoparticle Biosensors", Wiley Interdiscip. Rev. Nanomed. *Nanobiotechnol.* 2: 291–30, (2010).
- [7] Chen, C.L., Zhang, H., Ye, Q., Hsieh, W.Y., Hitchens, T.K., Shen, H.H., Liu, L., Wu, Y.J., Foley, L.M., Wang, S.J., Ho, C., "A new nano-sized ironoxide particle with high sensitivity for cellular magnetic resonance imaging", *Mol. Imaging Biol.*, 13: 825–839, (2011).
- [8] Konry, T., Bale, S., Bhushan, A., Shen, K., Seker, E., Polyak, B., Yarmush, M., "Particles and microfluidics merged: perspectives of highly sensitive diagnostic detection", *Microchim. Acta*, 176: 251–269, (2012).
- [9] Rügenapp, C., Gleich, B., Haase, A., "Magnetic nanoparticles in magnetic resonance imaging and diagnostics", *Pharm. Res.*, 29: 1165–1179, (2012).
- [10] Maier-Hauff, K., Ulrich, F., Nestler, D., Niehoff, H., Wust, P., Thiesen, B., Orawa, H., Budach, V., Jordan, A., "Efficacy and safety of intratumoral thermotherapy using magnetic iron-oxide nanoparticles combined with external beam radiotherapy on patients with recurrent glioblastoma multi for me", *J. Neurooncol.*, 103: 317–324, (2011).

- [11] Soenen, S.J.H., De Cuyper, M., "Assessing iron oxide nanoparticle toxicity in vitro: current status and future prospects", *Nanomedicine*, 5(8): 1261–1275, (2010).
- [12] Karlsson, H.L., Cronholm, P., Gustafsson, J., Moller, L., "Copper oxide nanoparticles are highly toxic: a comparison between metal oxide nanoparticles and carbon nanotubes", *Chem. Res. Toxicol*, 21 (9): 1726–1732, (2008).
- [13] Karlsson, H.L., Gustafsson, J., Cronholm, P., Möller, L., "Size-dependent toxicity of metal oxide particles—a comparison between nano- and micrometer size", *Toxicol. Lett*, 188 (2): 112–118, (2009).
- [14] Pandey, R.K., Prajapati, V.K., "Molecular and immunological toxic effects of nanoparticles", *Int. J. Biol. Macromol. Part A*, 107: 1278-1293, (2018).
- [15] Zhu, M.T., Wang, B., Wang, Y., Yuan, L., Wang, H.J., Wang, M., Ouyang, H., Chai, Z.F., Feng, W.Y., Zhao, Y.L., "Endothelial dysfunction and inflammation induced by iron oxide nanoparticle exposure: risk factors for early atherosclerosis", *Toxicol. Lett*, 203 (2): 162–171, (2011).
- [16] Mahmoudi, M., Simchi, A., Imani, M., Shokrgozar, M.A., Milani, A.S., Häfeli, U.O., Stroeve, P., "A new approach for the in vitro identification of the cytotoxicity of superparamagnetic iron oxide nanoparticles", *Colloids. Surf. B: Biointerfaces*, 75(1): 300–309, (2010).
- [17] Zhu, M.T., Feng, W.Y., Wang, Y., Wang, B., Wang, M., Ouyang, H., Zhao, Y.L., Chai, Z.F., "Particokinetics and extrapulmonary translocation of intratracheally instilled ferric oxide nanoparticles in rats and the potential health risk assessment". *Toxicol. Sci*, 107(2): 342–351, (2009).
- [18] Tang, Y.L., Guan, X.H., Wang, J.M., Gao, N.Y., Mc Phail, M.R., Chusuei, C.C., "Fluoride adsorption onto granular ferric hydroxide: effects of ionic strength, pH, surface loading, and major co-existing anions", *J. Hazard. Mater.* 171(1–3), 774–779. 2009.
- [19] Guan, X.H., Wang, J.M., Chusuei, C.C., "Removal of arsenic from water using granular ferric hydroxide: macroscopic and microscopic studies", *J. Hazard. Mater.* 156(1–3):178–185, (2008).
- [20] Baumann, J., Koser, L., Arndt, D., Filser, J., "The Coating Makes the Difference: Acute Effects of Iron Oxide Nanoparticles on *Daphnia magna*", *Sci. Tot. Environ*, 484: 176. (2014).
- [21] Zhu, H., Han, J., Xiao, J.Q., Jin, Y., "Uptake, translocation, and accumulation of manufactured iron oxide nanoparticles by pumpkin plants", *J. Environ. Monit*, 10: 713-717, (2008).
- [22] Zhu, X., Tian, S., Cai, Z., "Toxicity assessment of iron oxide nanoparticles in Zebrafish (*Danio rerio*) early life stages", *PLoS ONE*, 7(9): 462-486, (2012).
- [23] Hemaiswarya, S., Raja, R., Kumar, R.R., Ganesan, V., Anbazhagan, C., "Microalgae: a sustainable feed source for aquaculture", *World J. Microbiol. Biotechnol*, 27: 1737–1746, (2011).
- [24] Murdock, R.C., Braydich-Stolle, L., Schrand, A.M., Schlager, J.J., Hussain, S.M., "Characterization of nanomaterial dispersion in solution prior to in vitro exposure using dynamic light scattering technique", *Toxicol. Sci*, 101: 239–253, (2008).
- [25] Gurunathan, S., Han, J.W., Kim, E.S., Park, J.H., Kim, J.H., "Reduction of graphene oxide by resveratrol: A novel and simple biological method for the synthesis of an effective anticancer nanotherapeutic molecule", *Int. J. Nanomed*, 10: 2951–2969, (2015).
- [26] Sapsford, K.E., Tyner, K.M., Dair, B.J., Deschamps, J.R., Medintz, I.L., "Analyzing nanomaterial bioconjugates: A review of current and emerging purification and characterization techniques", *Anal. Chem.* 83: 4453–4488, (2011).
- [27] Taştan, B.E., Duygu, E., Donmez, G., "Boron bioremoval by a newly isolated *Chlorella* sp. and its stimulation by growth stimulators", *Water Res*, 46: 167–175, (2012).
- [28] Rippka, R., "Recognition and identification of cyanobacteria", *Methods in Enzymology*, 167: 28–67, (1988).
- [29] OECD, "Freshwater Alga and Cyanobacteria", Growth Inhibition Test. OECD Guideline for the testing of chemicals, Guideline 201, (2011).
- [30] Balusamy, B., Taştan, B.E., Ergen, S.F., Uyar, T., Tekinay, T., "Toxicity of lanthanum oxide (La₂O₃) nanoparticles in aquatic environments", *Environ. Sci.: Process. Imp*, 17: 1265-1270, (2015).
- [31] OECD, *Daphnia* sp., "Acute Immobilisation Test". OECD Guideline for the testing of chemicals, Guideline 202, (2004).
- [32] Porra, R.J., Thompson, W.A., Kriedemann, P.E., "Determination of accurate extinction coefficients and simultaneous equations for assaying chlorophylls a and b extracted with four different solvents: verification of the concentration of chlorophyll standards by atomic absorption spectroscopy", *Biochim. Biophys. Acta. (BBA) – Bioenergetics*, 975: 384–394, (1989).
- [33] Ip, P.F. Chen, F., "Production of astaxanthin by the green microalga *Chlorella zofingiensis* in the dark", *Process. Biochem*, 40: 733–738, (2005).
- [34] Kenney, J., Keeping, E. S., "Standard Error of the Mean in N. Princeton and V. Nostrand (eds.)", *Mathematics of Statistics*, 110: 132-133, (1951).
- [35] Jesus, J.R., Lima, J.S., Moura, O., Duque, G.S., Meneses, T. "Anisotropic growth of -Fe₂O₃ nanostructures", *Ceram. Int*, 44, 3585-3589, (2018).
- [36] Parsianpour, E., Gholami, M., Shahbazi, N., Samavat, F., "Influence of thermal annealing on the structural and optical properties of maghemite (γ-Fe₂O₃) nanoparticle thin films", *Surf. Interface Anal*, 47: 612–617, (2015).
- [37] Clogston, J.D., Patri, A.K., "Zeta potential measurement", *Methods Mol Biol*, 697: 63–70, (2011).
- [38] Ates, M., Daniels, J., Arslan, Z., Farah, I.O., "Uptake and toxicity of titanium dioxide (TiO₂) nanoparticles to brine shrimp (*Artemia salina*)", *Environ. Monit. Assess*, 185: 3339–3348, (2013).
- [39] Cheng, Lei., Luqing, Zhang., Kun, Yanga., Lizhong, Zhu., Daohui, Lin., "Toxicity of iron-based nanoparticles to green algae: Effects of particle size, crystal phase, oxidation state and environmental aging", *Environ. Pollut*, 218: 505-512, (2016).
- [40] Barhoumi, L., Dewez, D., "Toxicity of Superparamagnetic Iron Oxide Nanoparticles on Green Alga *Chlorella vulgaris*", *BioMed Res. Int*, <http://dx.doi.org/10.1155/2013/647974>, (2013).
- [41] Demir, V., Ates, M., Arslan, Z., Camas, M., Celik, F., Bogatu, C., Can, Ş.S., "Influence of Alpha and Gamma-Iron Oxide Nanoparticles on Marine Microalgae Species", *Bull. Environ. Contam. Toxicol*, 95(6):752-757, (2015).